JJMIE

Volume 10 Number 4, December. 2016
ISSN 1995-6665
Pages 253 - 261

Jordan Journal of Mechanical and Industrial Engineering

Two-Dimensional Analysis of Low Pressure Flows in the Annulus Region between Two Concentric Cylinders with Solid Fins

Wael Al-Kouz[a*], Suhil Kiwan[b], Aiman Alshare[c], Ahmad Hammad[c], Ammar Alkhalidi[d]

[a] *Mechatronics Engineering Department, German Jordanian University, Amman, 11180, Jordan*

[b] *Mechanical Engineering Department, Jordan University of Science and Technology, Irbid, 22110, Jordan*

[c] *Mechanical and Maintenance Engineering Department, German Jordanian University, 11180, Jordan*

[d] *Energy Engineering Department, German Jordanian University, 11180, Jordan*

Received August, 17, 2016 *Accepted November, 17, 2016*

Abstract

A finite volume code is used to solve for the steady-state two-dimensional laminar natural convection heat transfer for the gaseous low pressure flows in the annulus region between two concentric horizontal cylinders with an attached solid fin to the inner cylinder. Such flows can be found in the "evacuated" solar collectors and in the receivers of the solar Parabolic Trough Collectors (PTCs). Boussinesq approximation is utilized to model the buoyancy effect. It is found that Nusselt number (*Nu*) depends inversely on Knudsen number and directly on Rayleigh number. In addition, it is found that attaching a solid fin to the inner cylinder will enhance the heat transfer for such flows. Also, It is found that by increasing the tilt angle of the solid fin, then better heat transfer is achieved. Finally, it is concluded that by increasing the conductivity ratio, better heat transfer is gained.

Keywords: natural convection, heat transfer, low pressure, concentric cylinders, solar collectors, parabolic trough.

Nomenclature

C_p	Specific heat [J kg^{-1} K^{-1}]
D	Molecular diameter of the gas [m]
D_i	Inner annulus diameter [m]
D_o	Outer annulus diameter [m]
E	Energy flux on a surface per unit time
g	Gravity acceleration [m/s^2]
k	Thermal conductivity [W m^{-1} K^{-1}]
k_B	Boltzman constant= $1.38066\times10^{-23}\,JK^{-1}$
k_{eff}	Effective thermal conductivity [W m^{-1} K^{-1}]
Kn	Knudsen number
K_r	Fin thermal conductivity ratio
k_r	Effective thermal conductivity ratio (k_{eff} / k_f)
L	Length of the cylinder [m]
L_g	Gap Spacing between the two cylinders (r_o-r_i) [m]
$\overline{L_g}$	Dimensionless gap spacing between the two cylinders (r_o-r_i)/r_i
P	Pressure [Pa]
Pr	Prandtl number
Q	Heat transfer [W]
q_w	Local heat flux [W/m^2]
r_i	Inner annulus radius [m]
r_o	Outer annulus radius [m]
T	Temperature [K]
T_i	Temperature of annulus inner surface [K]
T_o	Temperature of annulus outer surface [K]
Ra	Rayleigh number ($g\beta(T_1$-$T_2)L^3/\alpha\nu$)
Ra_c	Rayleigh number based on L_c =($g\beta(T_1$-$T_2)L_c^3/\alpha\nu$)
Ra_i	Rayleigh number based on the inner diameter
Ra_m	Modified Rayleigh number
u	Velocity in x-direction [m/s]
v	Velocity in y-direction [m/s]
x, y	Cartesian coordinates [m]
x'	Line, starting from point a and ending at point b [m]
$\overline{X}$	Dimensionless $x' = \frac{x'}{r_o}$

Greek Symbols

α	Thermal diffusivity [m^2/s]
β	Thermal expansion coefficient [1/*K*]
λ	Molecular mean free path (m)
μ	Dynamic viscosity [kg m^{-1} s^{-1}]
ν	Kinematic viscosity [m^{2}s^{-1}]
φ	Angle as shown in Figure 1
ρ	Density of air, given by ideal gas equation (P/RT), [Kg/m^3]
σ	Lennard-Jones characteristic length (A^o)
σ_T	Thermal accommodation coefficient
σ_v	Momentum accommodation coefficient

* Corresponding author e-mail wael.alkouz@gju.edu.jo.

τ Tangential momentum

Θ Dimensionless temperature

Subscripts

eff Effective

f Fluid

F Fin

g Gap

i Inner

m Modified

n Normal

o Outer

r Ratio

1. Introduction

Rarefied and micro/nano flows have been studied extensively in the past two decades because of their relevance to the MEMS and NEMS devices as well as their wide applications found in the industry, such as aerospace, plasma and material processing applications [1; 2]. Recently, the whole world has started to depend on renewable energy as it produces no harmful pollutants to the environment and due to energy bill savings. Solar energy is one of the cleanest forms of renewable energy that is sustainable, inexhaustible, and inexpensive. In addition, solar energy is becoming more appealing as it can be gained without any restrictions. Researchers have investigated and developed technologies on how to harvest solar energy and to maximize the collection and utilization of solar energy. One of the most important applications for the rarefied flows that is related to the solar energy applications is the Parabolic Trough Collectors (PTCs) found in power plants. Since heat transfer analysis for PTCs is important for efficiency estimation of the power plant [3], this study aims to investigate the effect of attaching a fin to the inner cylinder on the flow and heat characteristics of the low pressure gaseous flow confined in the annulus region of two concentric cylinders. Also, the effect of Knudsen number and Rayleigh number on these characteristics will be addressed as well.

Rarefied flows can be classified by introducing Knudsen number (Kn). It represents the ratio of the mean free path (λ) to the characteristic length (L) of the geometry of interest.

Based on the study of Schaaf and Chambre [4] and that of Cercignani and Lampis [5], one can classify the flow regimes into four types: (i) Continuum regime if $Kn < 0.01$; (ii) Slip regime if $0.01 < Kn < 0.1$; (iii) Transitional regime if 1< *Kn* <10; and (iv) for $10 < Kn$, the free molecular regime. It is also worth to mention that in the slip flows, the slip boundary condition is applied at the surfaces and if the flow is non-isothermal, a temperature jump at the surface must be applied as well, while for the transitional and free molecular regimes, particle simulation methods, such as direct simulation Monte Carlo method, can be used to analyze the flow characteristics. For example, the supersonic gaseous flows into nanochannels using the unstructured 3-D direct simulation Monte Carlo method had been studied by Gatsonis *et al*. [6]. It was shown that the flow and heat transfer characteristics are affected by inlet Mach number (*Ma*), inlet pressure and the aspect ratio of the channel.

Similarity method is another technique that was utilized to solve for the flow and heat characteristics for continuum and rarefied flows. For instance, Kiwan and Al-Nimr [7] used the power law along with the similarity solution to solve for the flow and heat characteristics of a flow over a stretched microsurface. Also, Kiwan and Al-Nimr [8] used the same technique (similarity) to investigate the flow and heat characteristics for boundary layer flows in microsystems. In addition, Al-Kouz *et al*. [9] investigated the flow and heat transfer for rarefied flows over stretched surfaces using the similarity solution as well.

Flow in the region between two horizontally oriented concentric cylinders has been extensively studied experimentally and numerically in the past decades due to its relevance to parabolic trough solar collectors. The present paper provides further insight on the gaseous flow and heat transfer characteristics in the cavity of the annular region between two concentric cylinders, in which the inner cylinder is attached to a solid fin.

A comprehensive literature review for the computational and experimental investigations for the no-slip flow in the region of the annuli between two concentric cylinders is summarized by Kuehn and Goldstein [10; 11]. Moreover, Kuehn *et al*. [10] obtained a correlation using the conduction boundary layer model for the flow in the annulus region between to concentric horizontal cylinders. Raithby and Hollands [12] provided the following correlations for the conductivity ratio and length scale that is valid for $0.7 \le \Pr \le 6000$ and $Ra_c \le 10^7$ for the flow in the annulus region between two concentric cylinders:

$$k_r = \frac{k_{eff}}{k} = 0.386\left(\frac{\Pr}{0.861+\Pr}\right)^{1/4} Ra_c^{1/4} \quad (1)$$

where k_{eff} represents effective conductivity of the fictitious stationary fluid that will transfer the same amount of heat as the actual moving fluid, and L_c is given as follows:

$$L_c = \frac{2\left[\ln\left(r_o / r_i\right)\right]^{4/3}}{\left(r_i^{-3/5} + r_o^{-3/5}\right)^{5/3}} \quad (2)$$

Mack and Bishop [13] investigated the free convection in the annulus region between two concentric cylinders. In their study, they represented the stream function and the temperature variables using the third power of the Rayleigh number. The effects of Raleyigh number and radius ratio on the characteristics of the flow in the annuli of two infinite concentric cylinders using numerical techniques were studied by El-Sherbiny [14]. Rayleigh number was varied between 10^2 to 10^6, and the Radius Ratio, (RR) was taking the values between 1.25 and 10.

In his study, Mikhail A. Sheremet [15] investigated the effect of Ra, Pr, the inclination angle as well as the thermal conductivity ratio on the velocity and temperature fields of the laminar natural convection in an inclined cylindrical enclosure having finite thickness walls. The selected values for Rayleigh number were *Ra* = 10^4, 5×10^4, 10^5, while Prandtl number was varied to take the values of *Pr* = 0.7 and 7.0, the inclination angle values were 0, π/6, π/3, π/2 and the thermal conductivity ratio values of 5.7×10^{-4} and 4.3×10^{-2} is selected. The results show that it is possible

to indicate two intervals with a maximum magnitude of the generalized heat transfer coefficient at various values of the inclination angle of the tube and the analyzed range of Rayleigh number while the increase in Prandtl number is reflected in a delay in the thermal stabilization zone. It was also shown that for a certain range of the Rayleigh number less than 1×10^5, the thermal component of the natural convection is dominant while for Rayleigh number greater than 1×10^5 the hydrodynamic component of natural convection is the dominant.

Bouras *et al*. [16] developed a finite volume code to solve for the governing equations resulted from the Boussinesq approximation and the velocity stream function formulation to investigate the effect of Prandtl number as well as Rayleigh number for the natural convection in the annulus space between two elliptical confocal cylinders. It was found that the heat transfer increases as the Rayleigh number increases. Low Rayleigh numbers makes the conduction heat transfer dominant while high Rayleigh numbers makes the convection heat transfer dominant. They also concluded that for low Rayleigh numbers there is no effect for Prandtl number on the heat transfer but for higher Rayleigh numbers increasing Prandtl number increases the heat transfer.

The effect of fin conductivity ratio, Darcy number and Rayleigh number on the average Nusselt number for porous fins attached to the inner cylinder of the annulus between two concentric cylinders were investigated by Kiwan *et al*. [17]. They found that the heat transfer is enhanced for the case of a porous fin, also it was found that for porous fin, unlike the solid fins, the heat transfer decreases by increasing the inclination angle of the fin. Bouras *et al*. [18] numerically investigated the double diffusive natural heat transfer convection in the annular space between confocal elliptic shape enclosures using a finite volume code to solve the governing equations. They found that both heat and mass transfer increase with increasing Rayleigh number. Furthermore, the iso-concentrations exhibit a plume as iso-therms at large Rayleigh numbers. The plume diffuse throughout the annular space since the Lewis number is greater than one.

The natural convection heat transfer of nanofluids in annular spaces between horizontal concentric cylinders was investigated by Cianfrini *et al*. [19]. They developed two empirical equations based on a wide variety of experimental data and used them for evaluation of the nanofluid effective thermal conductivity and dynamic viscosity, while the other effective properties are calculated based on the mixing theory. Different conditions, such as the diameter of the particles was considered in calculated the heat transfer enhancement due to the nanoparticles dispersion in the liquid, and they concluded that there is an optimum particle loading for the maximum heat transfer.

Chamissem *et al*. [20] investigated the effect of Rayleigh number for natural convection in annular space flows. They found that there is a possibility to get a multi-cellular flows if the enclosure impedes movement of the fluid even if the Rayleigh number is small. They found an interval of large Rayligh numbers where the relaxation coefficients do not only affect the speed of calculation convergence but also the solution of the transfer equation. The effect of the relaxation coefficients on the solution is not valid beyond this interval. In the case of very large Rayleigh numbers, the stream function takes two values just before the divergence of the solution, this is very clear for the cases where symmetry boundary conditions is in the vertical direction.

The parabolic trough solar receiver is one of the applications for the flow in the annulus region between two horizontal concentric cylinders. The heat transfer of this application was analyzed by Padilla *et al*. [21]. They validated their model by comparison to Sandia National Laboratory (SNL) parabolic trough solar collector test (SEGS LS-2) in which the inner diameter of the receiver is 70 mm while the outer diameter is 115 mm. Based on their model they presented correlations for the heat transfer in the parabolic trough solar receiver.

Al-Kouz *et al*. [22] investigated the low-pressure flows in the annulus region between two concentric cylinders; they studied the effect of rarefaction on the flow and heat characteristics of such flows. In addition, a correlation for the conductivity ratio was proposed for such flows.

Vacuum pressure that operates the receivers of the parabolic trough collectors and the evacuated tube collectors is related to the operating temperature and the mean free path can be found in [1; 2] as:

$$\lambda = \frac{k_B T}{\sqrt{2}\pi d^2 P} \tag{3}$$

where k_B is the Boltzmann constant, T the temperature, P the pressure, d is molecular diameter of the gas under investigation and λ is the mean free path.

In the present work, a finite volume numerical Computational Fluid Dynamics (CFD) solution utilizing Boussinesq approximation is used to obtain the solution for the natural convection heat transfer characteristics between two concentric horizontal cylinders. The inner cylinder is attached to a solid fin and is subjected to a constant high temperature while the outer cylinder is held at constant lower temperature. Prandtl number (Pr) is taken to be constant and is equal to 0.701. Effects of Knudsen number (Kn), Ralyeigh number (Ra), fin inclination angle and the conductivity ration on the flow and heat transfer characteristics are investigated.

2. Mathematical Formulation

2.1. Governing Equations

In the present study, a steady-state, two dimensional, and laminar flow is investigated. Boussinesq approximation is utilized to account for the buoyancy force and all fluid properties are considered constant.

Figure (1.a) shows one of the most relevant applications to our study, namely the receiver of the parabolic trough collectors. Fig (1.b) illustrates the geometry of the flow in the annulus region between the two concentric cylinders in which the inner cylinder is attached to a solid fin. In the present study, the slip and temperature jump boundary conditions were imposed at the boundaries and the slip flow regime is investigated.

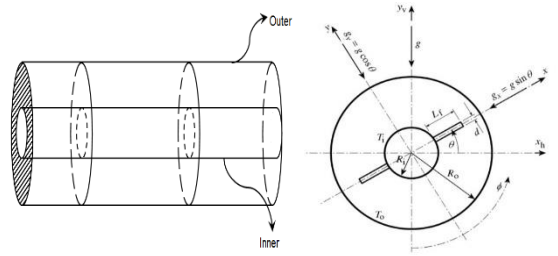

(a) (b)

Figure 1. (a) Parabolic trough receiver, (b) The geometry used for the computational domain, the annular region between two concentric cylinders with a solid attached fin

The governing equations that describe the problem under investigation are summarized below:

Conservation of mass:

$$\frac{\partial u}{\partial x}+\frac{\partial v}{\partial y}=0 \tag{4}$$

x-momentum:

$$\rho u\frac{\partial u}{\partial x}+\rho v\frac{\partial u}{\partial y}=-\frac{\partial P}{\partial x}+\rho g_x+\mu\left[\frac{\partial^2 u}{\partial x^2}+\frac{\partial^2 u}{\partial y^2}\right] \tag{5}$$

Note that the *x* component of the gravity is not equal to zero since there is a rotation for the solid fin that is attached to the inner cylinder of the annulus.

y-momentum:

$$\rho u\frac{\partial v}{\partial x}+\rho v\frac{\partial v}{\partial y}=-\frac{\partial P}{\partial y}-\rho g_y+\mu\left[\frac{\partial^2 v}{\partial x^2}+\frac{\partial^2 v}{\partial y^2}\right] \tag{6}$$

Energy:

$$\rho C_p u\frac{\partial T}{\partial x}+\rho C_p v\frac{\partial T}{\partial y}=k\left[\frac{\partial^2 T}{\partial x^2}+\frac{\partial^2 T}{\partial y^2}\right] \tag{7}$$

To estimate the fluid density, the ideal gas state equation is provided as an input:

$$\rho=\frac{P}{RT} \tag{8}$$

The boundary conditions applied are the slip and temperature jump at the inner and outer walls of the annulus, reported by Karniadakis *et al*. [1], Lockerby *et al*. [23] and Colin [24] as follows:

$$u_w-u_g=\left(\frac{2-\sigma_v}{\sigma_v}\right)\lambda\frac{\partial u}{\partial n}\approx\left(\frac{2-\sigma_v}{\sigma_v}\right)K_n\left(u_g-u_c\right) \tag{9a}$$

$$v_g=0 \tag{9b}$$

$$T_w-T_g=\left(\frac{2-\sigma_T}{\sigma_T}\right)\frac{2\gamma}{\gamma+1}\frac{k}{\mu c_v}\lambda\frac{\partial T}{\partial n}\approx\left(\frac{2-\sigma_T}{\sigma_T}\right)\frac{2\gamma}{\gamma+1}\frac{k}{\mu c_v}K_n\left(T_g-T_c\right) \tag{9c}$$

In equations (8a) and (8b), u_c and T_c represent the tangential velocity and temperature of the first cell from the wall in the computational domain. σ_v and σ_T represent the momentum and thermal accommodation coefficients and used as an inputs in the simulations, where:

$$\sigma_v=\frac{\tau_i-\tau_r}{\tau_i-\tau_w} \tag{10}$$

Where τ_i represents the tangential momentum of incoming particles to a certain surface (wall) and τ_r represents the tangential momentum of the reflected particles from that surface. While, τ_w is the tangential momentum of reemitted molecules from the surface with a temperature equal to the surface (wall) temperature:

$$\sigma_T=\frac{dE_i-dE_r}{dE_i-dE_w} \tag{11}$$

where dE_i is the energy flux of the incoming particles on a surface per unit time, dE_r represents the energy flux of the reflected particles per unit time, and dE_w denotes the energy flux of all the incoming particles that had been reemitted with the energy flux corresponding to the surface temperature T_w.

The corresponding Knudsen number (*Kn*) is defined as follows:

$$Kn=\frac{\lambda}{L_g} \tag{12}$$

where L_g is the gap spacing between the inner and outer cylinders.

Thermal boundary conditions are imposed at $r=r_i$ and r_o such that:

At $r=r_i$, $T=T_i$ (13)

At $r=r_{out}$, $T=T_o$ (14)

where T_i is the hot surface temperature and T_o is the cold surface temperature.

The local heat flux at the is calculated using Fourier's law of conduction at the surfaces of the inner cylinder and the fin as follows:

$$q_F=-k\frac{\partial T}{\partial n}\Big|_F \tag{15}$$

and $q_i=-k\frac{\partial T}{\partial n}\Big|_i$ (16)

Since the problem is steady, the heat transfer from the inner to the outer wall is calculated by integrating the local heat flux along the wall of the inner cylinder and the fin:

$$Q=\sum(\int_{A_i}q_i dA_i+\int_{A_F}q_F dA_F) \tag{17}$$

Then, the average heat transfer coefficient along the walls of the inner cylinder and the fin is calculated by combining equations 15, 16 and 17:

$$\bar{h}=\frac{Q}{(T_i-T_o)A_T} \tag{18}$$

From equation 19, the average Nusselt number can be calculated.

Price *et al*. [25] and Thomas [26] investigated the flow in the parabolic trough solar collector receiver, they lower the pressure in the annulus to a value that is less than one Torr, they found out that the resulting pressure for the free molecular regime in which Knudsen number is greater than 10 is approximately 0.013 Pa.

The present work aims to analyze the flow and heat characteristics for the slip flow regime in the annulus region between two horizontal concentric cylinders in which the inner cylinder is attached to a solid fin using two-dimensional computational model.

3. Numerical Solution

A finite volume analysis is utilized as a method of solution for the problem under investigation. The SIMPLE algorithm adopted from Versteeg and Malalasekera [27] and Patankar and Spalding [28] is used to calculate the pressure field. A hybrid second order accuracy scheme of central and upwind difference is used to differentiate the convective terms. The discretized equations are solved and the criterion of convergence is assumed when the maximum of the normalized absolute residual across all nodes is less than 10^{-6}.

4. Grid Independency

Fig. 2 shows a sample of the grid of the domain of the problem. It consists of a simple two-dimensional mesh. For the initial mesh, the grid step sizes are increasing in the radial and azimuthal directions with expansion factors of 1.06 and 1.15, respectively and then the adaptive grid technique is used. The chosen expansion factors are selected in order to capture the steep gradients near the solid-fluid interface and to better resolve the changes in the boundary layer. A systematic change was adopted to arrive at used factors as we have started with a uniform mesh and varied these parameters to a suitable level. Further change in these parameters will have no impact on the solution. In the adaptive grid technique, the velocity gradients near the walls are calculated and additional cells were added in order to reduce the velocity gradients below a certain value. A grid independency test is carried out by monitoring the heat transfer per unit length, and many solutions were obtained for different numbers of grid nodes. It was observable that there is a certain number of nodes in which any further increase of the nodes will not change the value if the heat transfer per unit length as can be seen in Table.1. It is clear from the table that the solution is mesh-independent for a grid of 80×480 in the radial and azimuthal directions, respectively. This grid size is used for all cases of *Ra*.

Table 1: Grid independent study

Mesh	Q(W/m)	Percentage change compared to 80x480 mesh
40×360	44.924	2.0196
60×360	44.2394	0.46493
80×360	43.989	-0.10365
80×480	44.0347	0

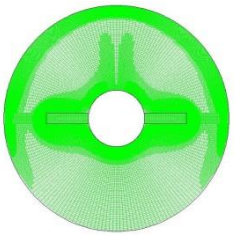

Figure 2 Adaptive grid system technique used in the simulations

5. Code Verification

To verify the numerical code, results of the current code are tested and compared with the results obtained by [10]. Fig. 3 illustrates a comparison between k_r obtained by the current code and that obtained by [10]; it should be noted that K_{eff} represents the thermal conductivity of the fluid, the verification utilized $Ra = 5.3\times10^4$. The comparison shows an error of less than 1.3 %. Also, Kiwan and Khodier [29] presented other validation studies using the same code for an open-ended channel partially filled with an isotropic porous medium.

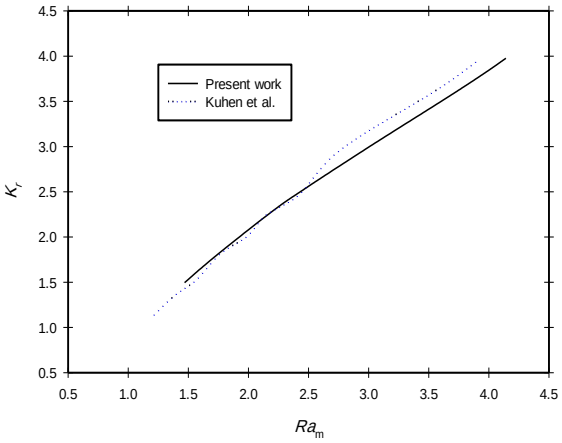

Figure 3. Comparison between current data and Kuhen et al. data

6. Results and Discussion

Fig 4(a) shows the velocity stream function contours. Knudsen number values of 0.01, 0.03, 0.05, 0.08 and 0.1 are considered. It is obvious from the graph that as Knudsen number increases, the center of rotation moves upward in the counter clockwise direction, this can be justified because of the rarefaction effect; the increase in rarefaction will increase the slip flow at the walls. Also, by increasing the mean free path, the interaction between molecules will be reduced and thus lower resulting velocities are obtained.

Fig. 4(b) illustrates the temperature contours (Isotherms) for different Knudsen numbers. The contours show that for all cases, the lower part of the annuli represents a case of a dominant conduction mode of heat transfer while in the upper part of the annulus; the convection mode is becoming dominant. One can see that for the lower part of the annulus that is in the region of 0 and 30 degrees counter clockwise, the flow is thermally stable while in the region between 70 and 90 degrees counter clockwise, the flow becomes unstable due to the buoyancy effects. It is also clear from the graph that as Knudsen number increases then the distortion and mixing of the flow decreases and consequently the heat transfer decreases.

  - Volume 10, Number 4 (ISSN 1995-6665)

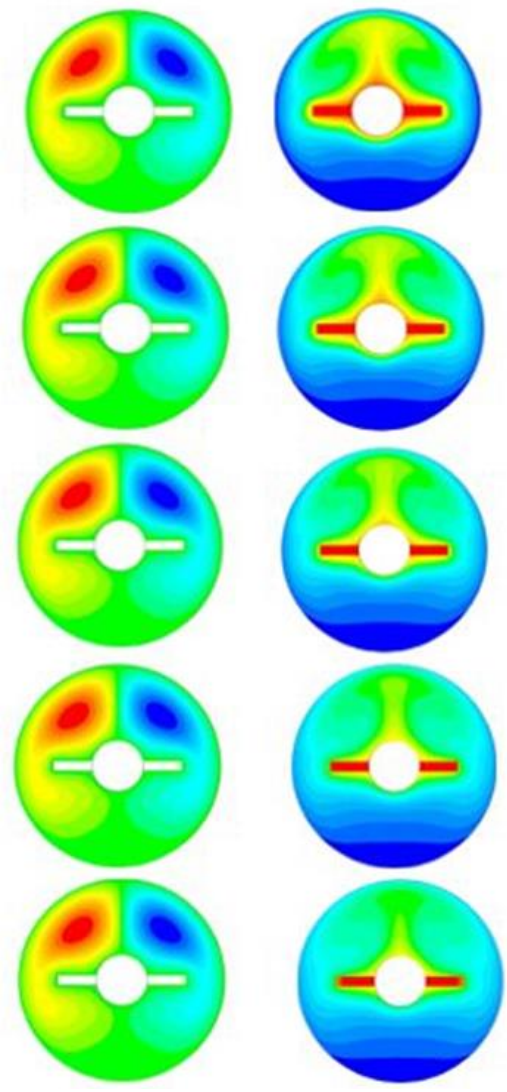

(a) (b)

Figure 4. (a) Streamlines [θ=0o], (b) Isotherms [θ=0o]

In Fig. 5, the temperature contours (isotherms) and the velocity stream function contours are plotted for different fin inclination angles. The graph shows for inclination angle θ=90^o, there are two symmetric circulation loops. As the fin inclination angle decreases, one of these loops is shifting upward while the other one is shifting downward. This shift increases the resistance to the flow. The maximum resistance is achieved for the case of angle θ=0^o. This case represents the minimum circulation velocity and the maximum thermal boundary layer thickness along the upper faces of the fins and the inner cylinder

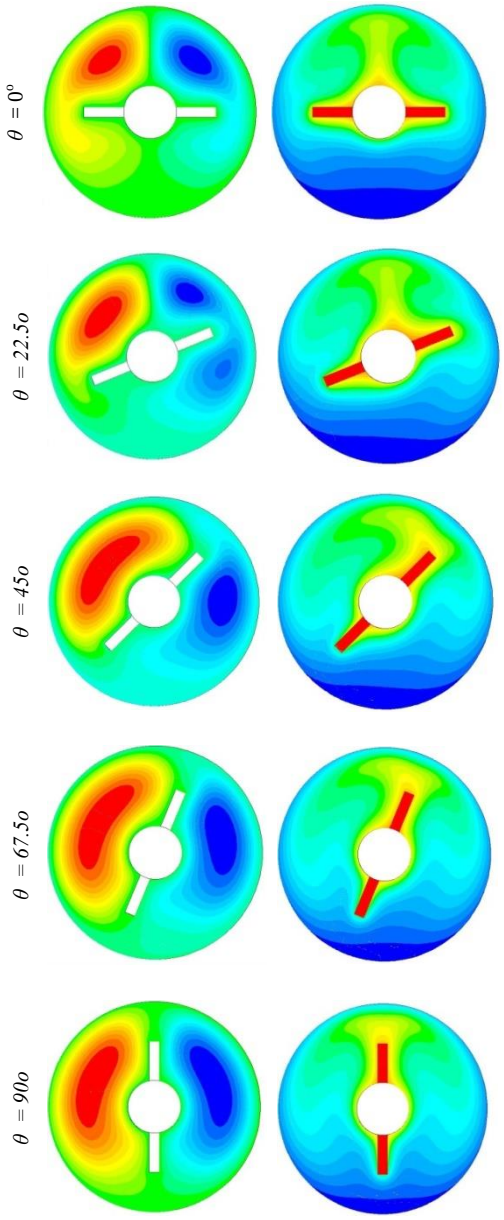

(a) (b)

Figure 5. (a) Streamlines for various fin inclination angles, (b) Isotherms for various fin inclination angles

Shown in Fig. 6, the variation of the local heat transfer coefficient *h* with the angle φ for both cases of the slip and no slip flows whether the inner cylinder is attached to a fin or not. The graph shows that by attaching a fin then the local heat transfer is higher than the case of the no fin for both of the slip and no-slip flows. Also, the graph shows that the slip flow will reduce the local heat transfer coefficient compared to the no slip flow case. Moreover, the graph illustrates that the local heat transfer coefficient will increase by increasing the value of angle φ for both of the slip and the no slip flows whether the inner cylinder is attached to a fin or not.

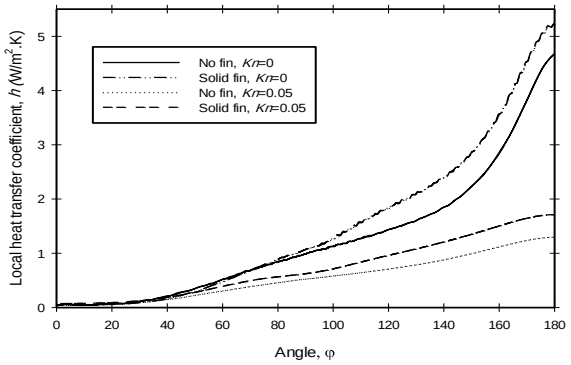

Figure 6. Variation of the local heat transfer coefficient for the cases of no fins and with fins for continuum and rarefied flows along the angle (φ).

Fig. 7 demonstrates the dimensionless vertical velocity V_y variations with the dimensionless radial distance r^* for different values of Knudsen numbers that cover the slip flow regime.it is obvious from the graph that the higher the Knudsen number, the lower dimensionless vertical velocity for cases where r^* is less than one. The opposite will occur for the cases where r* is higher than unity, the higher Knudsen number will result in lower dimensionless vertical velocity. This will result in less heat transfer and consequently lower Nusselt number.

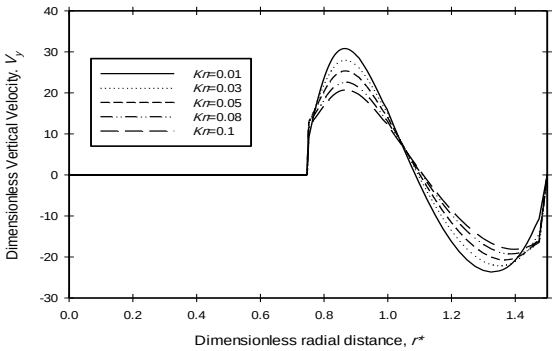

Figure 7. Variation of the dimensionless vertical velocity (V_y) with the dimensionless radial distance (r^*) for different Knudsen numbers

In Fig. 8, the dimensionless temperature distribution T^* is plotted against the dimensionless radial distance r^*, the graph shows that as Knudsen number increases then the temperature jump at the outer cylinder surface will increase.

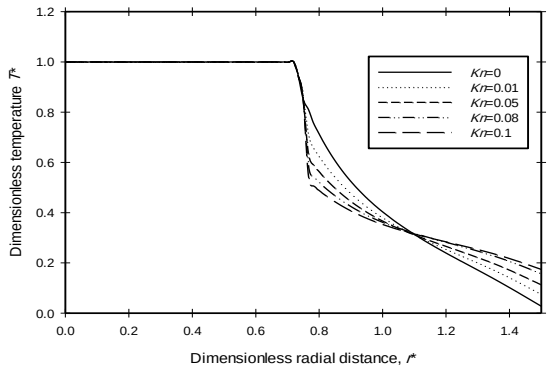

Figure 8 Variation of the dimensionless temperature (T^*) with the dimensionless radial distance (r^*) for different Knudsen numbers

The variation of the average Nusselt number with Rayleigh number for different Knudsen numbers is shown in Fig. 9. The graph illustrates that as Rayleigh number increases then the average Nusselt number is increasing for the same Knudsen number. Also, the graph shows that as Knudsen number increases, the average Nusselt number decreases for the same Rayleigh number. In addition, the graph shows that for low Rayleigh numbers, the dominant mode of heat transfer is conduction while for higher Rayleigh numbers, the convection heat transfer will dominate.

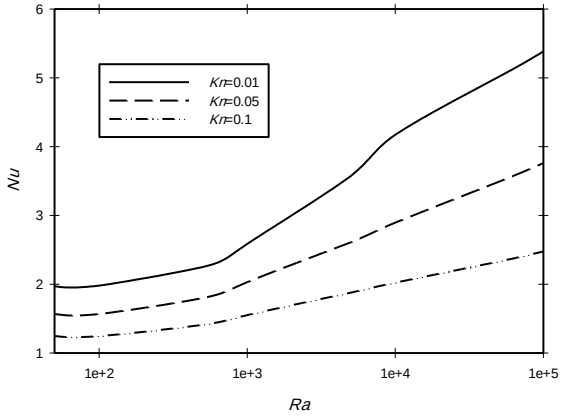

Figure 9. Variation of Nusselt number (*Nu*) with Rayleigh number (*Ra*) for different Knudsen numbers

Variations of the average Nusselt number with the conductivity ratio of the fin for different values of Knudsen number are plotted in Fig. 10. The graph shows that by increasing Knudsen number, then the average Nusselt number will decrease for the same conductivity ratio. In addition, it is obvious that as the conductivity ratio increases, the average Nusselt number increases up to a certain limit beyond which a further increase in the conductivity ratio has no significant effect on the average Nusselt number.

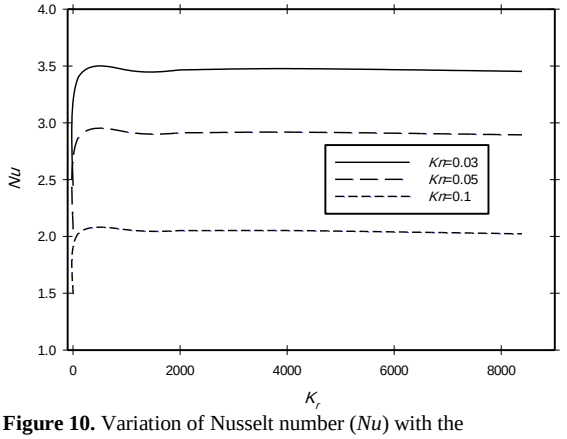

Figure 10. Variation of Nusselt number (*Nu*) with the conductivity ratio (*Kr*) for different Knudsen numbers

Figure 11 shows the average Nusselt number variations with the fin inclination angle, the graph shows that for the no slip and slip flows and for the region where θ is in the range of 0-20 degrees, the average Nusselt number is almost constant. Beyond this range, the higher the fin inclination angle, the higher the average Nusselt number. The graph also shows that there is almost an order of

magnitude difference in the value of Nusselt number between the continuum versus the slip flow case.

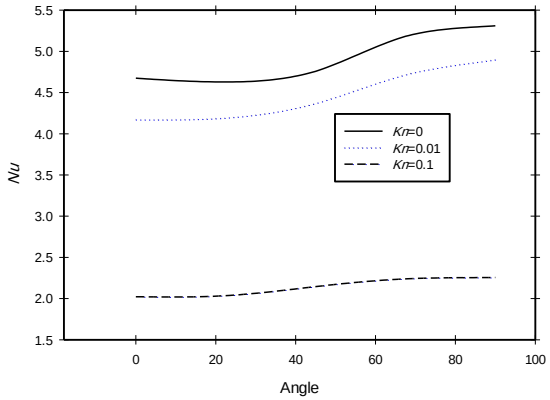

Figure 11 Variation of Nusselt number (*Nu*) with the fin inclination angle (θ) for different Knudsen numbers

7. Conclusions

A steady, two-dimensional analysis of low-pressure gaseous laminar flow in the annulus region between two concentric cylinders in which the inner cylinder is attached to a solid fin is carried out. This type of flow has a wide variety of applications such as the receiver of the parabolic trough collectors and the evacuated tube collectors. Rarefaction effects on both flow and heat characteristics of such flows are investigated. It is found that as Knudsen number increases, the slip velocity and the temperature jump at the boundaries will increase. In addition, it is found that as Knudsen number increases, the average Nusselt number will decrease. Moreover, it is found that by attaching a fin to the inner cylinder for such flows, average Nusselt number will increase for the same Knudsen number. Finally, It is concluded that no-slip (Continuum) flows have better heat transfer characteristics (measured by the average Nusselt number) than slip flows.

References

[1] Karniadakis G, Beskok A, and Aluru N. *Microflows and Nanoflows*. Springer; 2005.

[2] Bird G A. *Molecular Gas Dynamics and the Direct Simulation of Gas Flows*. Oxford Univ: Press Oxford; 1994.

[3] Patnode AM. *Simulation and Performance Evaluation of Parabolic Trough Solar Power Plants*. Master thesis. University of Wisconsin-Madison: College of Engineering; 2006.

[4] Schaaf S, Chambre P. *Flow of Rarefied Gases*. Princeton Univ: Press Princeton; 1961.

[5] Cercignani S, Lampis M. *Rarefied gas dynamics*. New York: Academic Press; 1974.

[6] N.A. Gatsonis, W. Al-Kouz, R.E. Chamberlin, ‘‘Investigation of rarefied supersonic flows into rectangular nanochannels using a three-dimensional direct simulation Monte Carlo method’’ . Physics of Fluids. Vol. 22, No. 1-16, 2010.

[7] S. Kiwan, M.A. Al-Nimr, ‘‘Flow and heat transfer over a stretched microsurface’’. ASME transaction J. Heat Transfer, Vol. 28, No. 6, 2009, 1-8.

[8] S. Kiwan and M.A. Al-Nimr, ‘‘Investigation into the similarity for boundary layer flows in micro-systems’’. ASME transaction; J. Heat Transfer, Vol. 132, No. 4, 2010, 1-9.

[9] W. Al-Kouz, M. Sari, S. Kiwan and A. Alkhalidi, ‘‘Rarefied flow and heat transfer characteristics over a vertical stretched surface’’. Journal of Advances in Mechanical Engineering. Vol 8(8), 2016, 1-13.

[10] T.H. Kuehn, R.J. Goldstein, ‘‘An experimental and theoretical study of natural convection in the annulus between horizontal concentric cylinders’’. J. Fluid Mech, Vol. 74, 1976, 695-719.

[11] T.H. Kuehn, R.J. Goldstein., ‘‘Correlating equations for natural convection heat transfer between horizontal circular cylinders’’. Int J. Heat MassTransfer., Vol. 19, 1976, 1127-1134.

[12] G.D. Raithby, K.G. T. Hollands, ‘‘A general method of obtaining approximate solutions to laminar and turbulent free convection problems”. Advances in Heat Transfer, No. 11, 1975, 265-315.

[13] L.R. Mack, E.H. Bishop, ‘‘Natural convection between horizontal concentric cylinders for low Rayleigh numbers’’. Q.J. Mech. Appl. Math. XXI, 1968, 223-241.

[14] A. El-Sherbiny, ‘‘Natural convection in air layers between horizontal concentric isothermal cylinders’’. Alexandria Engineering Journal, Vol. 43, No. 3, 2004, 297-311.

[15] M.A. Sheremet, ‘‘Laminar natural convection in an inclined cylindrical enclosure having finite thickness Walls’’. International Journal of Heat and Mass Transfer, Vol. 55, 2012, 3582–3600.

[16] A. Bouras, M. Djezzar, C. Ghernoug, ‘‘Numerical simulation of natural convection between two elliptical cylinders: Influence of Rayleigh number and Prandtl number”. Energy Procedia, Vol. 36, 2013, 788-797.

[17] S. Kiwan, O. Zeitoun, ‘‘Natural convection in a horizontal cylindrical annulus using porous fins’’. International Journal of Numerical Methods for Heat & Fluid flow, Vol. 18, 2008, 618-634.

[18] A. Bouras, M. Djezzar, H. Naji, C. Ghernoug. ‘‘Numerical computation of double-diffusive natural convection flow within an elliptic-shape enclosures’’. International Communications in Heat and Mass Transfer, Vol. 57, 2014, 183-192.

[19] M. Cianfrini, M. Corcione, A. Quintino, ‘‘Natural convection heat transfer of nanofluids in annular spaces between horizontal concentric cylinders’’. Applied Thermal Engineerin, Vol. 31, 2011, 4055-4063.

[20] W. Chmaissem, S. Suh, M. Daguenet, ‘‘Numerical study of the Boussinesq model of natural convection in an annular space: Having a horizontal axis bounded by circular and elliptical isothermal cylinders’’. Applied Thermal Engineering, Vol. 22, 2002, 1013-1025.

[21] R. Padilla, G. Demirkaya, D. Goswami, E. Stefankos, ‘‘Heat transfer analysis of parabolic trough solar receiver’’. Applied Energy, Vol. 88, 2011, 5079-5110.

[22] W. Al-Kouz, A. Alshare, A. Alkhalidi, S. Kiwan, ‘‘Two dimensional analysis of low pressure flows in the annulus region between two concentric cylinders’’. SpringerPlus, 2016, 5-529

[23] D. Lockerby, J. Reese, R. Barber, ‘‘Velocity boundary condition at solid wall in rarefied gas calculations, Physical Review E’’. Vol. 70, No. 1, 2004, 017303.

[24] Stéphane Colin, *''Heat Transfer and Fluid Flow in Minichannels and microchannels: Single-phase gas flow in microchannels''.* Elsevier Ltd 2006.

[25] H. Price, E. Lupfert, D. Kearney, E. Zarza, G. Cohen, R. Gee, ''Advances in parabolic trough solar power technology''. J Solar Energy Eng Tran ASME, Vol. 124, No.2, 2002, 109-25.

[26] Thomas JR, "*Heat conduction in partial vacuum''.* Virginia Polytechnic Institute and State University. Blacksburg, Virginia: U.S. Department of energy, EM-78-C-04-5367, 1979.

[27] H. Versteeg, W. Malalasekera, *''An Introduction to Computational Fluid Dynamics: The Finite Volume Method*''. Prentice-Hall, Essex, 1995.

[28] S.V. Patankar, D. B. Spalding, ''A calculation procedure for heat, mass and momentum transfer in three-dimensional parabolic flows''. Int. J. of Heat and Mass Transfer, Vol. 15, No. 10, 1972, 1787-1806.

[29] S. Kiwan, M. Khodeir, ''Natural convection heat transfer in an open- ended inclined channel partially filled with porous media''. J. Heat Transfer Engineering, Vol. 29, 2008, 67-75.